Journal of Basic and Applied Engineering Research
p-ISSN: 2350-0077; e-ISSN: 2350-0255; Volume 2, Issue 22; October-December, 2015, pp. 1929-1935

http://www.krishisanskriti.org/Publication.html

Numerical Investigation of the Effect of Apex Flap Deflection on the Flow Field over Double Delta Wing

Vasanthan.K[1], Soumalya DasGupta[2] and Kashyap Sathyamurthy[4]

School of Aeronautical Sciences
[1,2,3]B.Tech Hindustan University, Chennai
E-mail: [1]k7vasanth@gmail.com, [2]soumalyadasgupta@gmail.com, [3]kashy_a@yahoo.com

Abstract—*The double delta wing produces vortex which contribute to the overall stability of aircraft. At a higher angle of attack the vortex breakdown occurs thus creating anomalies of aerodynamic forces & moments. Methods have been developed for an improved endurance of the vortex. This paper presents the numerical analysis of the effect of apex deflection on the flow field over a double delta wing of 90/60 sweep configuration with a rounded leading edge at a Reynolds number of* $1.5*10^5$ *per metre for three apex deflection of 0, 10, 20 degree in the negative incidence. The K-ω SST turbulence model is opted to carry out the flow analysis using the commercial software FLUENT.*

Keywords*: double delta wing, vortex control, apex deflection, strake wing vortex.*

1. INTRODUCTION

There has been a perpetual desire for increased speed, manoeuvrability and efficiency ever since the modernization of military aircrafts which have broken the “sound barrier” and made supersonic regime plausible. Clearly, due to the complexity of the flow fields associated with this, it draws more attention and requires deeper understanding. One such efficient way is by using delta or double delta wings which can delay the stalling at very high angle of attack. Over the past decades, extensive aerodynamic research has been carried out in double delta wing that has facilitated aircraft designs that incorporate swept wings and highly swept wings with leading edge extensions (LEX). Technological advancements which generate high-lift and low drag forces with regard to fighter aircraft at high angles of attack have been solicited especially in order to maintain their superiority through superior manoeuvrability. At large angle of incidence, the flow field around a slender body is dominated by vortices generated on the fore body, leading edge extensions, wings, and control surfaces. Since majority of the time spent by all high speed aircraft is at subsonic speeds and since their supersonic capability exists for short “supersonic dashes”, the discussion involving delta wing is zeroed down to low speed, incompressible flow.

1.1 Flow Phenomenon

Every case of three dimensional flows over swept wings is a unique one and hence it is difficult to generalize. This is due to arious design parameters which could characterize a wing viz. aspect ratio, taper ratio, sweep angle, thickness, and camber and twist distribution. Nevertheless, one of the most important parameters which classify the wing is the mean sweep angle. Majority of combat aircraft have sweep angle of about 300-500, and hence the analysis of such flow if of greatest relevance.

Flow over swept wings is of a highly complex three dimensional natures, comprising an inextricable mixture of shock waves, vortex systems, strong span wise flows, and boundary-layer separation and reattachment. The “typical” flow pattern over a moderately swept wings at moderate AOA is shown in fig 1.1. High velocities occur locally near the leading edge, as the AOA is increased for a given Mach number. Flow separation takes place at subsonic speeds, rolling up to form a part-span vortex.

1.1.2 Double Delta Wing Vortex Characteristics

The double delta wing is essentially a delta wing with a 'kink' in its leading edges. The kink forms the shoulder where the leading edges of the strakes (or LEX) and main wing intersect. The geometry of these wings further complicates the flow field structure due to the presence of a pair of coherent vortices produced by the strake and main wing leading edges.

The strake vortices beyond the kink tend to remain fairly constant as they are no longer being fed energy from flow separation over the main wing. They typically move outboard and closer to the surface of the wing. The main wing vortices are more highly energized and tend to move inwards and away from the surface of the wing.

Flow over a double delta wing is very similar to that over a single delta wing, but much more complicated. The flow in the leeward side separates and rolls up into a pair of coherent, counter rotating vortices. If the leading edge is sharp, the flow will separate along its entire length. The vortex emerging at the apex of the strake is known as strake vortex. Another vortex, called the wing vortex, is produced at the kink i.e. strake/wing junction. The leading-edge vortex, which is characterized by high velocities and low static pressure, increases in diameter and intensity as the core follows a path downstream and inboard at an angle slightly greater than the sweep angle. As the wing's angle of attack increases, the vortex axial and rotational velocities increase and the vortex core height above the wing increases and start moving inboard. Primary vortex generation is nearly independent of Reynolds number due to the extremely small effective length, or radius of curvature, of the leading edge. However, high Reynolds number flow does decrease vortex diameter because it effectively adds energy and velocity to the core resulting in a more tightly wrapped core. The primary vortex pair creates lateral, outboard boundary layer flow on the wing surface, which collides with the primary separation and results in additional separation and a corresponding secondary vortex pair formation. The secondary vortex pair is weaker, is located outboard and rotates in a direction opposite to the primary vortices. Unlike the primary pair, the secondary vortex pair's strength and size are dependent on Reynolds number.

Flow over the double delta wing mainly depends on many factors such as Reynolds number, Mach number, leading edge radius, kink angle, sweep angle, platform of strake, various fillet shapes and many other factors. Unfortunately, there are limits to the benefits produced by the delta/double-delta wing vortices.

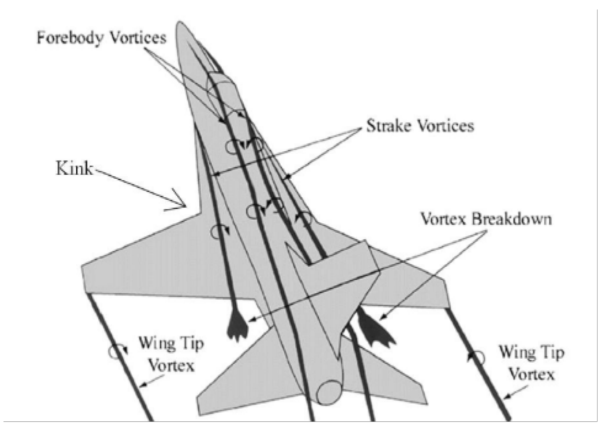

Fig. 1.1: Flow Field over Double Delta Wing Aircraft

2. MODEL DETAILS

Double Delta (65^0-90^0) wing which were decided to be used are drawn in GAMBIT. The dimensions of all three models are same except for the angle of deflection being 0, 10, 20 degree in the negative incidence. Dimensional details are given in Fig. 5.1.

- The wing is basically flat plate bevelled at an angle of 20 degree.
- The models have chord length of 735 mm.
- The wingspan is 250 mm.
- The thickness of wing is 15mm.
- The thickness of apex strake is 6.5 mm.
- The wing tip has been replaced by an apex strake at 23% chord.
- Domain created is C-H model type.

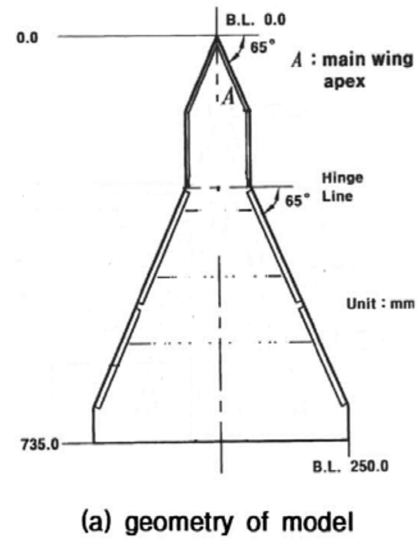

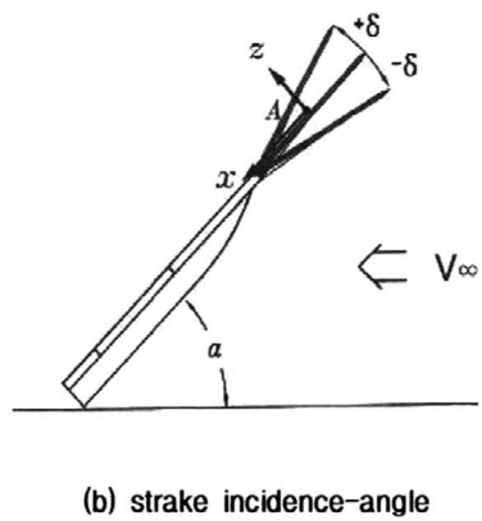

Fig. 2.1: Dimensional details of Wing (a) Geometry of Wing (b) Strake-incidence angle

2.1 Mesh Details

The first step towards the CFD is meshing which is done using GAMBIT. The later steps of simulating the ow around the model and the post processing is done using FLUENT software. FLUENT uses Finite Volume Method to solve the governing equations of uid mechanics. The design of the model can be imported using Neutral files of various Industry Standard Formats such IGES, Parasolid, etc., formats.

`Face' termed in GAMBIT and FLUENT is basically a surface constructed by joining edges or lines. The `Make Tolerant' option assigns a default tolerance value to each imported vertex and edge to maintain the topological integrity for the geometry. `No Stand Alone Faces' option deletes the imported vertices, edges and/or faces which are not connected to higher topology. In GAMBIT, the geometric entities are designated as vertex, edge, face and volume, which define a complete geometry. Real entities possess their own geometrical description, that is, they are defined by mathematical formulae that describe their locations and shapes. Virtual entities do not possess their own geometrical descriptions; instead they derive their geometry by referencing to one or more real entities.

The flow volume is meshed by the default tetrahedral meshing scheme. The meshed volume is checked for the quality of the mesh. It is required to keep the geometry free from skewed elements otherwise it causes errors in FLUENT. The meshed geometry is exported from GAMBIT as a Mesh File which is then imported to FLUENT.

Table 2.1: Mesh details

MODEL	MODEL 1	MODEL 2	MODEL 3
No. of elements	1590160	1589768	1592352
Excellent 0-0.25	477048	476931	477706
Good 0.25-0.5	57246	57232	57325
Fair 0.5-0.75	1054848	1054588	1056302
Poor 0.75-0.9	1018	1017	1019

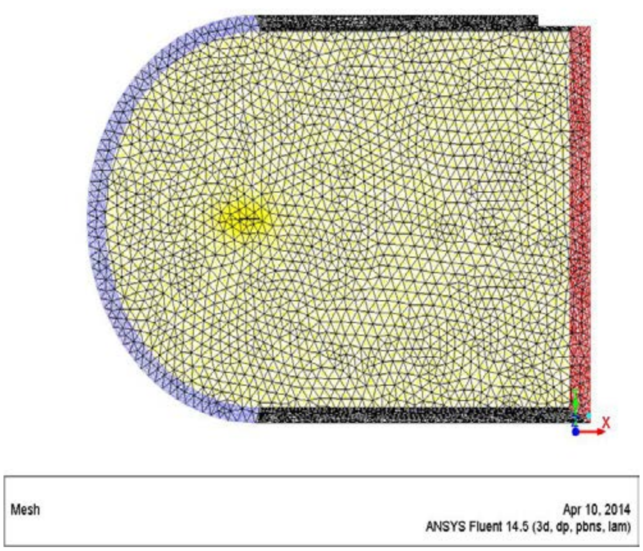

Fig. 2.2: Mesh of model in domain

(a) Model with zero deflection

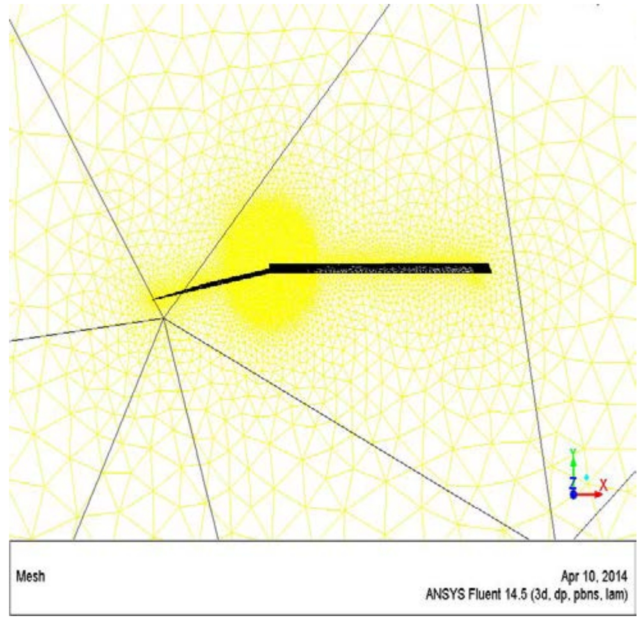

(b) Model with -10^0 deflection

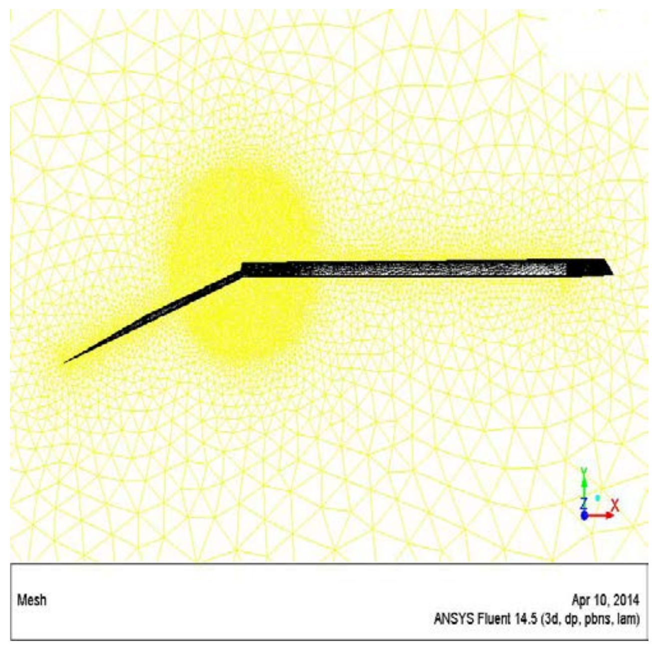

(c) Model with -20^0 deflection

Fig. 2.3 Zoom-in view of Model Mesh

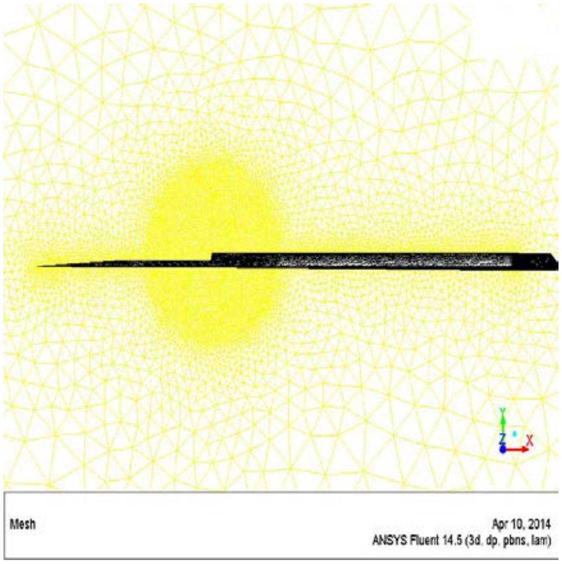

2.2 Simulation Details

Simulation of the uid ow in FLUENT requires an understanding of the problem itself. It is this understanding of the problem that leads to the answer for various question about which solver, viscous model, boundary conditions etc. to be selected.

In this research, default pressure based, implicit, segregated solver is used.

- Solver: Pressure based

For Pressure-based Solver, the pressure equation is derived from the continuity and momentum equations such that the velocity field, corrected by the pressure satises the continuity.

- Type of algorithm: Seggregated

The segregated or decoupled type algorithm solves the governing equations sequentially while in the coupled type the governing equations are solved simultaneously. Segregated algorithm is memory efficient, however the convergence of the solution is comparatively slow.

There are different models for simulating turbulent flow such as Spalart Allmaras, k-ε, k -ω, Reynolds Stress Model and Large Eddy Simulation Model. They differ in the number of equations that are used for solving turbulence.

- Type of Model: k-ω SST

k -ω models solves two additional transport equations (for the turbulence kinetic energy, k, and either the turbulence dissipation rate, ε, or the specific dissipation rate, ω). The SST model is a combination of the k-epsilon in the free stream and the k-ω models near the walls. It does not use wall functions and tends to be most accurate when solving the flow near the wall. The SST model does not always converge to the solution quickly, so the k-epsilon or k-omega models are often solved first to give good initial conditions.

Simulation of a fluid flow involves specifying boundary conditions. There are various boundary types available in FLUENT that specify the flow on the boundaries of the physical model. It is important to understand what boundary types should be specified depending on the problem statement.

- Type of Boundary condition: Velocity Inlet type

Velocity-Inlet boundary type allows to specify the inflow velocity by different methods, either by specifying the magnitude and direction or velocity magnitude normal to the boundary or velocity components. The fluid flow is solved for incompressible type as the Mach number to be considered is very low. Static temperature at the velocity inlet boundary can be set in the temperature field for simulations involving energy equation.

- No slip condition specified.

No slip wall condition is used for the boundary wall defining the aircraft geometry. The no slip condition causes a velocity gradient near the wall such that the velocity of the fluid at the stationary wall is zero and gradually increases until it reaches the free stream velocity.

- Symmetry boundary condition is used.

If the physical boundary and the expected pattern of the flow solution is symmetric, symmetric condition is used. This increases computational efficiency by reducing the simulation time as only half of the model is to be simulated. The interior of the flow volume is chosen as fluid representing air.

Monitoring the progress of the solution is essential and gives an indication whether the solution is converging or diverging.

Divergence of the simulation means that there is an error in setting up the problem such as the way the boundary conditions are defined or the model needs to be re-meshed with finer mesh. Convergence can be monitored from plotting the residuals for every iteration by `Residual Monitor'.

- Large fluctuations mean that the solver is unable to solve the flow volume domain and thus finer re-meshing should be considered.

3. COMPUTATINAL RESULTS

The three models are compared and the optimised. An attempt has been made to simulate three dimensional flow fields around the models taken. All the simulation are done using the commercial software FLUENT. The numerical results were generated using the K-ω SST turbulence model available with FLUENT. The basic flow field over the double delta wing models at subsonic speed was obtained. In order to study the effect of angle of attack and leading edge shape, a validation test was performed by referring to double delta wing reported in literature. The following section discusses in details all the results obtained from simulation.

- The aerodynamic force and moment coefficients for various angles of attack are presented in this section. The reference lengths used in the calculation of the aerodynamic coefficients are the chord length of 735 mm and wing span is 500 mm and the wing plan form area 0.21 m^2.

3.3.1 Variation of drag with change in α

The drag coefficient versus angle of attack is plotted in Fig. 6.1. Angle of attack is varied from 15 to 35 degrees. The drag coefficient versus angle of attack shows a parabolic curve, which indicates that the drag increases with the Square of the angle of attack.

Table 3.1: Variation of drag forces with Angle of Attack

AOA	0 deg	-10deg	-20deg
15	7.58E-05	7.34E-05	8.13E-05
20	1.39E-04	9.60E-05	1.26E-04
25	2.15E-04	2.03E-04	1.62E-04
30	3.35E-04	3.13E-04	2.86E-04
35	4.92E-04	4.68E-04	3.97E-04

3.3.2 Variations of lift with change in α

Lift coefficient as a function of angle of attack is plotted in the Fig. 3.2. The lift coefficient versus angle of attack gives a linear function of angle of attack with a positive slope, i.e. with the increase in the angle of attack the lift coefficient increases. Angle of attack is varied from 15 to 35 degrees.

Table 3.2: Variations of Lift forces with Angle of Attack

AOA	Model 1	Model 2	Model 3
15	2.41E-04	2.34E-04	2.32E-04
20	3.62E-04	2.35E-04	3.31E-04
25	4.56E-04	4.58E-04	3.41E-04
30	5.83E-04	5.77E-04	5.41E-04
35	7.15E-04	7.19E-04	6.23E-04

Fig. 3.3 shows the lift versus drag coefficient for change in angle of attack. It is clear from this Fig. that drag coefficient is proportional to square of lift coefficient which is in agreement with the theory.

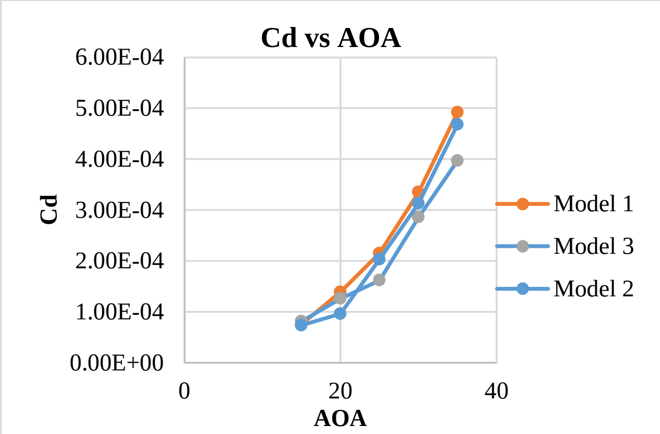

Fig. 3.1: C_d vs. α

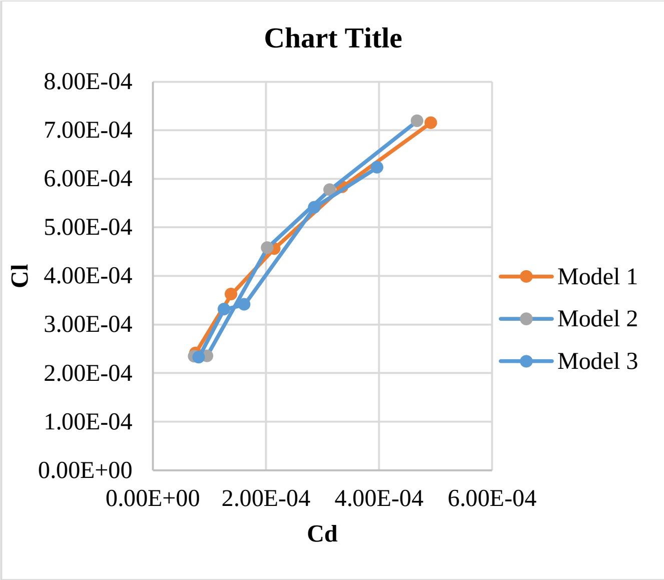

Fig. 3.2: C_l vs α

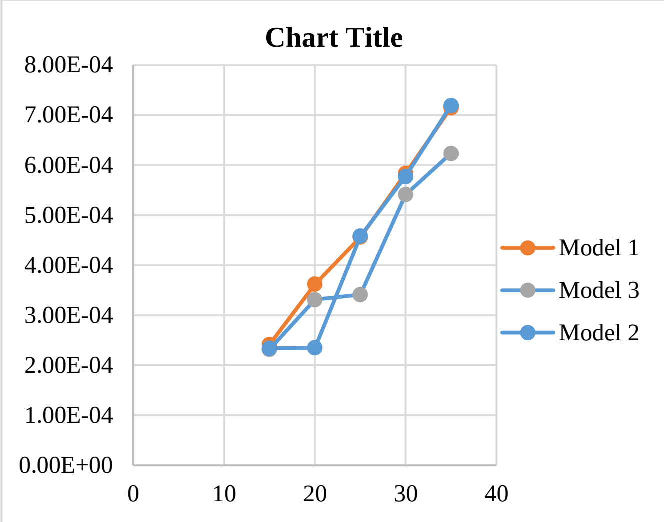

Fig. 3.3 C_l vs α

3.4 Effect of angle of attack

As angle of attack increases to 15 degrees, the suction side of the double delta wing becomes more dominant due to formation of strong strake vortex. Due to this at x/c=0.5 to 0.7 the Cp tends to increase in magnitude. Two peaks are obtained at a location of x/c=0.9. This may be due to the pressure of strake and wing vortices. The presences of strake & wing vortices are shown in Fig 3.4. Beyond this angle of attack the magnitude of pressure decreases. With increase of angle of attack, the strake and wing vortices start to coil around each other. As a consequence, the strake vortex moves closer to the wing surface and moves outboard.

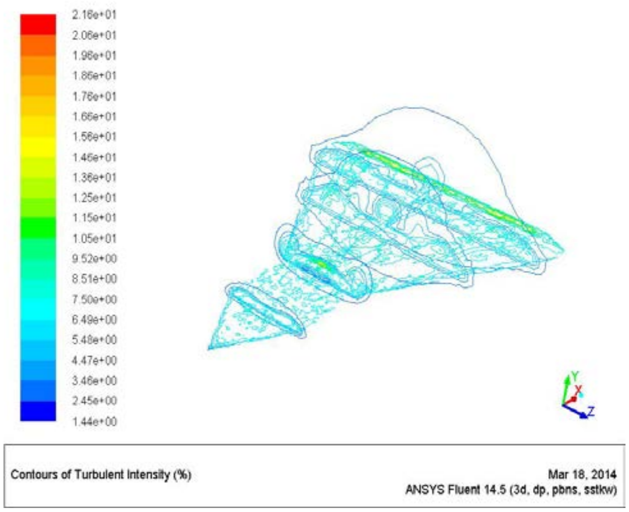

Fig. 3.4: Model with zero deflection at α=15^0

From Fig 3.5 we see at α=15^0 for model with δ=10°, it can be seen that the root chord centre line suction pressure has increased and also the wing vortex gains energy which can be seen by the rise in suction pressure. The effect of strake vortex is negligible. The maximum suction peak was found at x/c=0.6, further downstream the suction peak reduces.

Fig 3.6 shows at α=30^0 for model with δ=0°. At x/c=0.6 two peak can be observed, whereas at x/c=0.9 only one suction is seen. Here it can be observed that the strake vortex loses its energy further downstream of the wing.

3.4.1 Effect of apex deflection

a) δ=10°

It can be seen that all angle of attacks the strake vortex was not captured well. An important thing is to notice that the suction pressure increases for all angle of attack even beyond α=20^0 at typical location of x/c=0.8

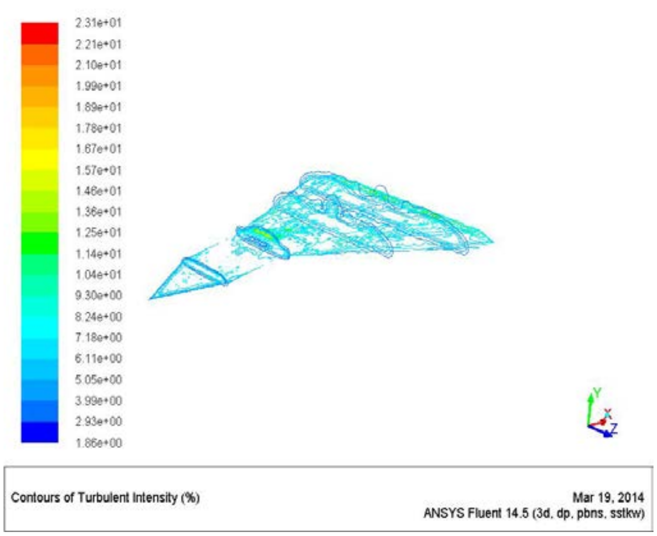

Fig. 3.5: α=15^0 for model with δ=10°

b) δ=20°

It can be seen that the vortex breakdown is delayed. However the suction pressure is much less when compared with model δ=10°. The following section gives us detailed description about the nature of unsymmetrical vortices & the effect of apex deflection to control the unsteady/vortex shedding.

It is seen that for model with apex deflection of δ=10° the suction peak of the wing vortices was maximum , compared with the model without apex deflection. Similar trend was found for α=35^0 at x/c=0.6.

At α=35^0, the weak strake vortex suction peak was not observed and the strong wing vortex suction peak is observed. As α increases from 10^0 to 30^0, the magnitude of strake and wing vortex suction peak increases. Beyond this angle the vortices lose their suction and hence the suction peak decreases. The strake and wing vortex suction peak beyond α = 20^0 appears to grow in an exponential fashion. It is seen that the value of Cp at the centre root chord of the wing for both the models with apex deflections of δ=10° & δ=20° are maximum when compared with model for δ=0°. At α=35^0 unsymmetrical vortex nature is observed which in turn leads to a phenomenon of vortex breakdown for model with δ=0°, weak strake vortex suction peak and the strong wing vortex suction peak is observed on the wing. The suction peak of the wing vortex is maximum for δ=10° when compared with the models δ=0° & δ=20°.

Magnitude of suction peak increases along the core as α increase and also along the downstream. From these figures the model with δ=10° & δ=20° has better Cp values than model with δ=0°.

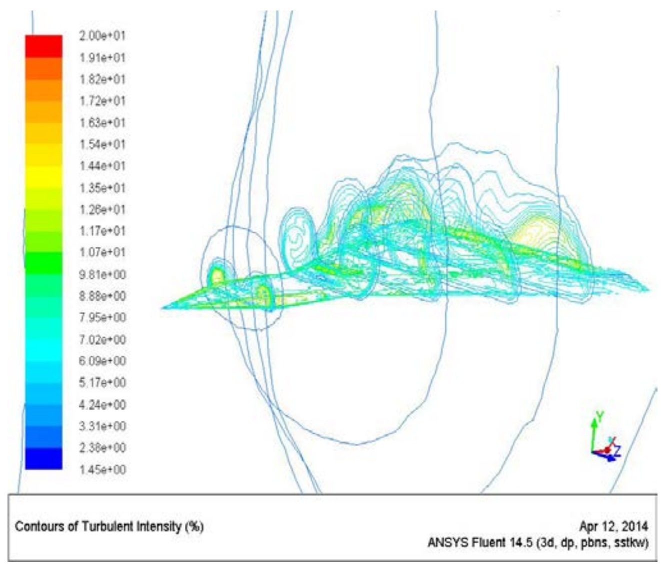

Fig. 3.6: α=30^0 for model with δ=0°

4. CONCLUSION

Computational investigation was made on three double delta wing models with different apex deflection angle of 0-deg, 10-deg & 20-deg. The entire tests have been carried out at velocity of 100 m/s (R_e =1.5*10^5). Effect of angle of attack and effect of apex deflection were obtained on double delta wing using experiments. The investigation was done in commercially available software FLUENT.

A numbers of important conclusion have been made from the present investigations that are summarized as follows:

From the results it is seen that apex deflection seems to be ineffective for low angles of attack. At higher angles of attack the normal force coefficient increases for model with apex deflection of $\delta=10°$. Apex deflection greater than 10° leads to a decrease in normal force. At low angles of attack, symmetric flow in the leeward side was observed for all models at low angle of attack. Apex deflection helps in delaying the vortex breakdown, however a limit to apex deflection has to be determined. At very high angle of attack, asymmetric nature of vortex were observed for $\delta=0°$ which was eliminated by the use of apex deflection. K-ω SST turbulence is well suited turbulence model for capturing most of the flow phenomenon.

REFERENCES

[1] Wang, J. J and Liu, J. Y., "The effects of apex flap on the leading-edge vortex breakdown of a cropped double delta wing", The Aeronautical Journal, November, 2003.

[2] Sohn, M. H., "Effect of apex strake incidence-angle on the vortex development and interaction of a double-delta wing", Exp Fluids, 48:565–575, 2010.

[3] N.G. Verhaagen "An Experimental Investigation of Vortex flow over delta and double delta wing at Low speed", (1983)

[4] Sheshagiri K. Hebbar, Max. F.Platzer and Feng-His Li "Visualization of Vortex flow over Delta Wing in Dynamic Motion", AIAA Journal, Vol.10 (2001)

[5] Sreenivasulu.J "Experimental and Computational Studies over a Double Delta Wing at Subsonic speeds", M.E Thesis, Birla Institute of Technology (June 2008)

[6] Kumar B., "Investigation of flow field on double delta wing with different leading edge shape at subsonic speed", M.E. Thesis, 2010.

[7] Polhamus, E. C., "A concept of the vortex lift of sharp-edge delta wings based on a leading-edge-suction analogy", NASA D-3767 (December 1966).

[8] M.J.Liu; Z.Y.Lu; C.H.Qiu; W.HSu; X.K.Gao; X.Y.Deng; S. W. Xion "Flow Patterns and Aerodynamic Characteristics of a Wing-Strake Configuration"

[9] Hugo A. Gonzalez, Gary E. Erickson, James H. Bell, Blair G. McLachlan, "Effects of Various Fillet Shapes on a 76/40 Double Delta Wing from Mach 0.18 to 0.7"

[10] Anderson, J. D "Fundamentals of Aerodynamics", ,Third edition, McGraw-Hill, 2001, pp. 398-415

[11] Freeman, J.A "Computational Fluid Dynamics Investigation of Vortex Breakdown for Delta Wing at High Angles of Attack", Air Force institute of Technology, Ohio (March 2005)

[12] Nath, B. Das, S. and Prasad, J.K., "Flow field study on a 65-deg blunted delta wing", National Conference on Wind Tunnel Testing 12-14 March 2007, Bangalore.

[13] Sohn, M. H. and Chang, J. W., "Effect of a center body on the vortex flow of a double-delta wing with leading edge extension", Aerospace Science and Technology-14, pp. 11–18, 2010.

[14] Polhamus. E.C "Prediction of Vortex Lift Characteristics by Leading Edge Suction analogy", Journal of Aircraft, Vol. 8, pp. 193-201 (1971)

[15] Hsu, C.H. and Liu, C.H., "Navier-stokes computation of flow around a round-edged double-delta wing", vol. 28, No. 6, AIAA Journal, June 1990.

[16] Nath.B "Flow field investigation over Delta Wing at Subsonic Speed" , M.E Thesis, Birla Institute of Technology, Mesra (June 2001)

[17] Al-Garni, A. Z. Saeed, F and Al-Garni, A. M., "Experimental and Numerical Investigation of 65-deg Delta and 65/40-deg Double-Delta Wings", Journal of Aircraft, Log Number: C10913.

[18] Lu, Feng-Hsi "Static and dynamic flow visualization studies of two double-delta wing models at high angles of attack" (1992)

[19] Wang, J. J and Qiang, Tu., "Effect of wing planform on leading-edge vortex structures", Chinese science bulletin**,** Hydromechanics, Vol.55 No.2, pp-120−123, January 2010.

[20] Young-Ki Lee, Heuy-Dong Kim "Vortical Flows over an LEX-Delta Wing at High Angles of Attack" (Korea) KSME International Journal, VoL 18, No. 12, pp. 2273-2283, (2004)

[21] Sukanta Saha, Bireswar Majumdar, "Modelling and Simulation on Double Delta Wing", (Jadavpur University) March 2013

[22] Evert G.M. Geurts "Low speed straked delta wing"

[23] Zuppardi G, Valenza "Visualizing Strake and Vortices in supersonic flow by a Thermographic Technique"

[24] C. W. Smith, J. N. Ralston, and H. W. Mann "Aerodynamic Characteristics of forebody and nose strakes on F-16 Wind tunnel experiments" NASA Contractor Report 3053

[25] Dhanvada M. Rao Vigyan Research Associates "VORTICAL FLOW MANAGEMENT FOR IMPROVE CONFIGURATION AERODYNAMICS", Hampton, VA 23666, U.S.A.

[26] David F. Fisher, Daniel G. Murri, Wendy R. Lanser "Effect of Actuated Forebody Strakes NASA F-18 HARV", NASA Technical Memorandum 4774 (1996)

[27] Jawahar Sivabharathy "Investigation of flow field around double delta wing with apex flap at subsonic speed" M.E Thesis (2010)

[28] Ajay Dev, "Performance Optimization of Double Delta Wing" (2013)

[29] Grismer, D.S and Nelson "Double Delta Wing Aerodynamics for Pitching moments with and without sideslip", Journal of Aircraft, Vol. 32, No. 6, Nov-Dec 1995

[30] Ray Whitford, "Design for Air Combat"

[31] Wirachman Wisnoe, Rizal Effendy Mohd Nasir, Wahyu Kuntjoro, and Aman Mohd Ihsan Mamat, "Wind Tunnel Experiments and CFD Analysis of Blended Wing Body (BWB) Unmanned Aerial Vehicle (UAV) at Mach 0.1 and Mach 0.3" Cairo, 2009

[32] S. K. Hebbar, M. F. Platzer, A. E. Fritzelas, "Reynolds number effects on the vortical-flow structure generated by a double-delta wing" (2000)

[33] Stefan Gortz, "Realistic Simulations of Delta wing Aerodynamics using Novel CFD Methods" (2005)